

A Study on Two-dimensional Spectrum Analysis System of Energy and Time

ZHANG Liuqiang, LI Yinglin, ZHANG Jian, YUAN Yuan

(Key Laboratory of Optoelectronic Technology and Systems, Ministry of Education, Chongqing University, Chongqing 400044, People's Republic of China)

Abstract: Proposed is a two-dimensional (2D) spectrum analysis system for acquiring the statistical information of radioactive particles on two dimensions, i.e. energy and time. Based on pulse width modulation readout circuit, such a system with 4-channels is designed, which converts the radiation signal into a rectangular pulse signal with pulse width modulated. The pulse width, occurrence time, and pulse count of the rectangular pulses are measured simultaneously with digital counters, so that the 2D spectra on energy and time of the radioactive particles can be obtained efficiently based on bi-parameter statistical analysis. A prototype of this 2D system is tested with gamma rays from ^{241}Am isotopes, from which both the correlated 2D spectra and the independent spectra on energy and time are obtained. The energy spectra of four channels shows all characteristic peaks of ^{241}Am gamma rays, among which the full-energy peak at 59.5keV exhibits energy resolution of about 5-6%, suggesting a good energy resolution and channel uniformity of the system. The regression of the time spectra of the characteristic peaks can give the time constants of each characteristic peak, revealing the time characteristics of the nuclear reactions in the radiative source.

Keywords: Energy Spectrum, Time Spectrum, Two-dimensional Spectrum, Pulse Width Modulation, Gamma Ray

1 Introduction

In the field of radiation detection, with the development of high-speed analog-to-digital converter (ADC) and programmable digital processing chips, the technology of digital spectrum analysis system has achieved rapid progress, enabling the high-speed acquisition, processing and analysis of particle or photon pulse signals [1-5]. The performance of the existing energy spectrum analysis systems, however, usually depends on high-speed and high-precision ADCs. Large number of ADC devices used for arrayed detectors not only increases the volume and cost of the system, but also adds a lot of redundant data, causing difficulties in system control and data processing.

The traditional spectrum analysis systems usually test the pulse amplitude and pulse time separately. Due to the difference of the two parameters, it is necessary to convert the pulse signal into different waveforms processed later in separated channels, which increase the complexity of circuit [1-4]. In addition, peak-holding circuits are often adopted for multi-channel amplitude detection, so that it is impossible to test the pulse amplitude and pulse time simultaneously [5-7]. So far, for the existing multi-channel energy-and-time (2D) spectrum analysis systems, the problems such as the complexity of readout circuit and the efficiency of data processing have never been solved.

In this paper, proposed and tested is a four-channel energy-and-time spectrum analysis

system, which converts the probed pulse signals from the preamplifiers into rectangular pulses, of which the pulse width is proportional to the amplitude of the probed pulse signals (corresponding to the particle energy), while the rising edge represent the generation time of the probed pulse signals (corresponding to the particle occurrence time). The rectangular pulses are quasi digital pulse signals that can be directly input to a field-programmable gate array (FPGA) system for digital processing and statistical analysis that gives the particle energy and occurrence time simultaneously. The energy-and-time 2D spectrum analysis system performs the pulse time and pulse width measurement using finite state machine technique and outputs correlated 2D spectrum data based on the bi-parameter statistics of pulse count. The system not only enables the 2D spectrum analysis on energy and time, but also achieves a high resolution without using ADC devices, thus it provides a novel technique for the development of high-performance spectrum analysis systems and spectral imaging systems.

2 2D Spectrum Analysis System

2.1 System Design

The framework of energy-and-time 2D spectrum analysis system for a 2×2 pixel array detector is shown in Fig.1.

The photons or particles emitted from a radiation source produce in the detector a weak electric current pulse, which is amplified, filtered, and formed by the front-end analog circuit, then converted, by a fixed

threshold comparator, into a rectangular pulse with pulse width modulation. The processed signal is then analyzed by a FPGA system to measure the pulse width (corresponding to the particle energy) and the time interval (corresponding to the duration between two successive particles). The merged data of four channels is stored in the first in, first out (FIFO) memory, and then transmitted through the USB data bus to a host computer, which is responsible for data acquisition control, spectrum mapping, and file management.

The FPGA chip of the system adopts low-cost and low-power FPGA device, EP4CE10F17C8 of Altera Cyclone IV E series, which has 10k logic elements and 130 I/O ports, with clock frequency up to 400 MHz and core voltage of 1.2V. The USB chip adopts the Cypress USB 2.0 Microcontroller, CY7C68013A of EZ-USB FX2LP™, working in Slave FIFO mode, with data transmission rate up to 53Mbps. The PC software is designed using C# language, and it can perform 4-channel data acquisition and control, spectral mapping and smoothing, statistical analysis and file management.

2.2 Principle of Waveform Transformation

The front-end analog circuit first transforms the exponential decay pulse from the charge-sensitive amplifier into a quasi-Gaussian pulse to reduce the impact of noise, then transforms the quasi-Gaussian pulse into a quasi-triangular pulse using an integral circuit with constant current discharge, and finally converts the quasi triangular pulse into a rectangular pulse with a fixed threshold comparator^[8-10]. To avoid

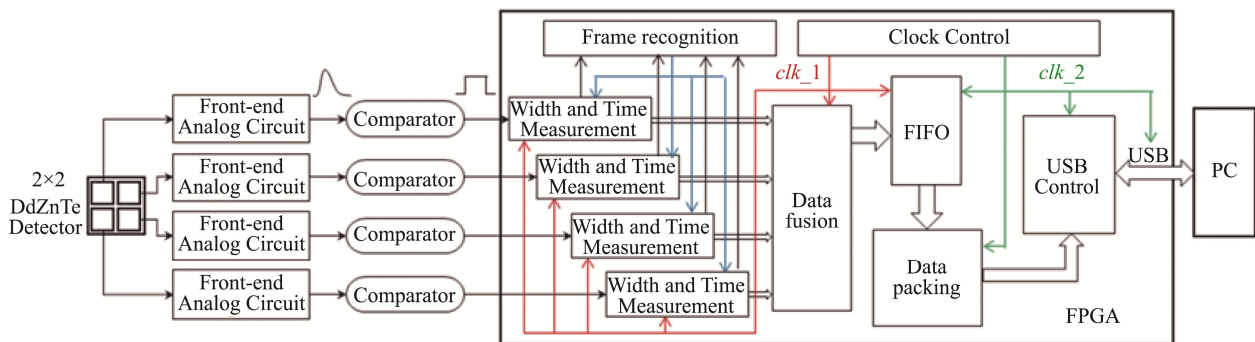


Fig.1 The Block Diagram of the 2D Spectra System for Energy and Time Analysis

the influence of noise, hysteresis comparators are adopted with high and low threshold, i.e. the comparator outputs high level when the signal voltage is above the high threshold, and vice versa. As a result, the digital rectangular pulse, which has a linear relationship between its pulse width and the corresponding amplitude of the original signal, is obtained through quasi-triangle pulse shaping and set-threshold comparison.

Fig.2(a) shows the principle of the waveform transformation based on hysteresis comparator, and Fig.2(b) shows the actual signal waveforms, among which the blue curve is the input quasi-triangle pulse signal and the green curve is the output rectangular pulse signal.

2.3 Method for Measuring Pulse Time and Pulse Width

The measurement of rectangular pulses is performed in a FPGA system using a state machine with five states, and two counters are used to measure the pulse time and pulse width respectively. The transition relationship of the states is shown in Fig.3.

- In Judge state, the rising edges of the signal are under continuous testing, and the state machine will jump to the Count 1 state immediately if a rising edge is detected; otherwise, the state continues.

- In Count 1 state, counter 1 and 2 keep counting when the signal is at a high level. If the value of counter 1 is equal to 16 (equal to a time of $0.16 \mu\text{s}$ as the clock frequency is 100MHz), a frame

identification pulse signal “FrameStart” will be generated and transferred to the frame recognition module just for a normal nuclear event. It will immediately jump to the Count 2 state when the falling edge of the signal is detected.

- In Count 2 state, counter 1 clears, and counter 2 continues to count until the second rising edge of the input signal is detected, then counter 2 is reset after its count value is stored in “data1”, and the state machine jumps to Count 3 state.

- In Count 3 state, counter 1 and 2 keep counting, frame identification as in the Count1 state is performed first, and then the state machine jumps to Out state when a falling edge comes.

- In Out state, the write flag “writeflag” and the output data “dataout” are send out to the next process module. The “dataout” includes the 4-digit channel number of time data, the time data of the upper 12 bits of “data1”, the 4-digit channel number of width data, the width data of the count value of counter 1. At last, the state machine jumps to Count 2 state immediately to complete a measurement.

In the experiments, the pulse width has a range of 0-40 μs , and the relative pulse time has a range of 0-80 ms, which is 2000 times of the former. In order to use a single clock frequency, counter 1 has a digit width of 12 bits, and counter 2 has a digit width of 23 bits, but only the high 12 bits are used for output. As a result, the two counters have the same output count range of 0~4095, but the corresponding time range is different.

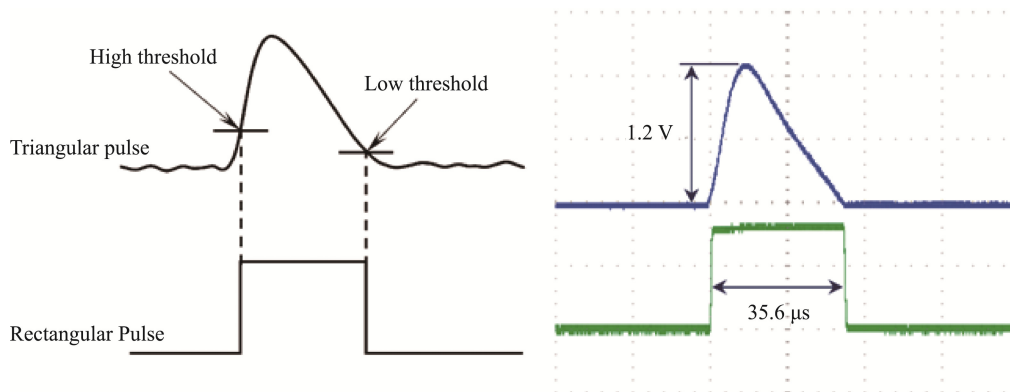


Fig.2 The Principle of Signal Conversion and the Actual Waveforms in Experiment

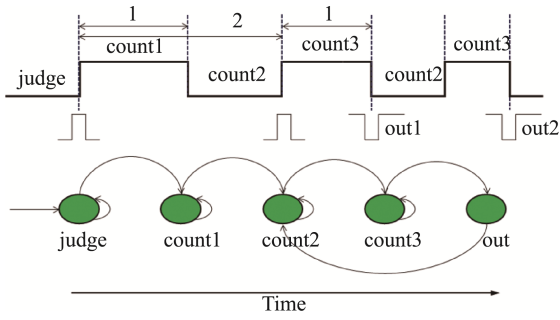


Fig.3 The State Machine for Pulse Time and Pulse Width Measurement

When the clock frequency is 100 MHz, the pulse width measurement takes a range of 0~40.95 μs and an accuracy of 10 ns; while the pulse time measurement takes a range of 0~83.87 ms and an accuracy of 20.48 μs ; both covering the time range of the experiment.

3 Experiment and Data Analysis

3.1 Independent Spectrum Test

In Fig.4, (a), (b), (c), (d) show the energy spectra of readout channel 1, 2, 3, 4 respectively, and (e), (f), (g), (h) show the time spectra of readout channel 1, 2, 3, 4 respectively. All characteristic peaks of ^{241}Am gamma rays are clear in the energy spectra, including a full energy peak ($\text{Am } \gamma$ 59.5keV) and several lower energy peaks (N_pL_α 13.4keV, N_pL_β 16.8/17.8keV, N_pL_α 20.8keV,

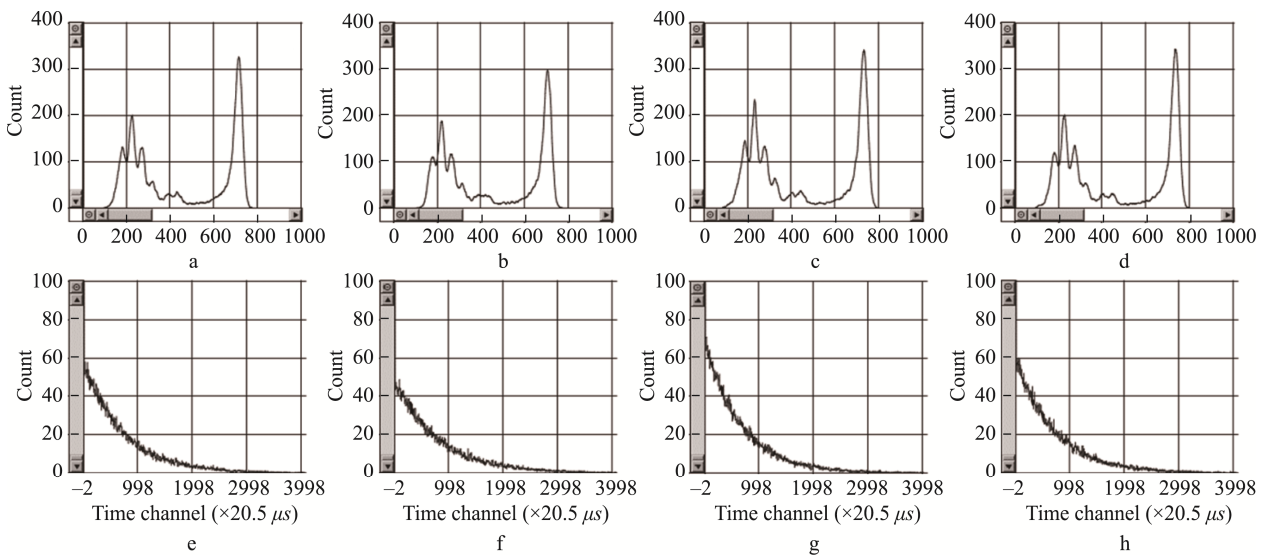


Fig.4 The Energy and Time Spectra of ^{241}Am Gamma Rays

$\text{Am } \gamma$ 26.3keV, $\text{Am } \gamma$ 26.3keV) [11-12]. The full energy peak is located near energy channel 730, with energy resolution of about 5-6%. The time spectra are basically exponential decay curves, which agrees approximately with the theory of Poisson distribution.

To compare the spectra of four readout channels, the four curves are merged together as shown in Fig.5. It can be seen that both the address and the maximum count of the full energy peaks deviate from each other slightly.

Table 1 summarizes the statistical results of the energy spectrum of four channels. It is obvious that the total photon count for each channel is exactly the same, while the count and address of the full energy peak are slightly different. The full energy peaks have full-width-at-half-maximum (FWHM) all around 40, with energy resolution of 5.8%, 6.0%, 5.7% and 5.3%, respectively. Note that the deviation of channel 2 is more significant than others, which means that the performance of pixel 2 is worse than other pixels. However, since the spectrum data of each channel does not make any correction, considering the difference between detector pixels and readout circuits, the results actually indicate that the 2D spectrum analysis system for the 2x2 pixel array detector can achieve high energy resolution as well as good consistency.

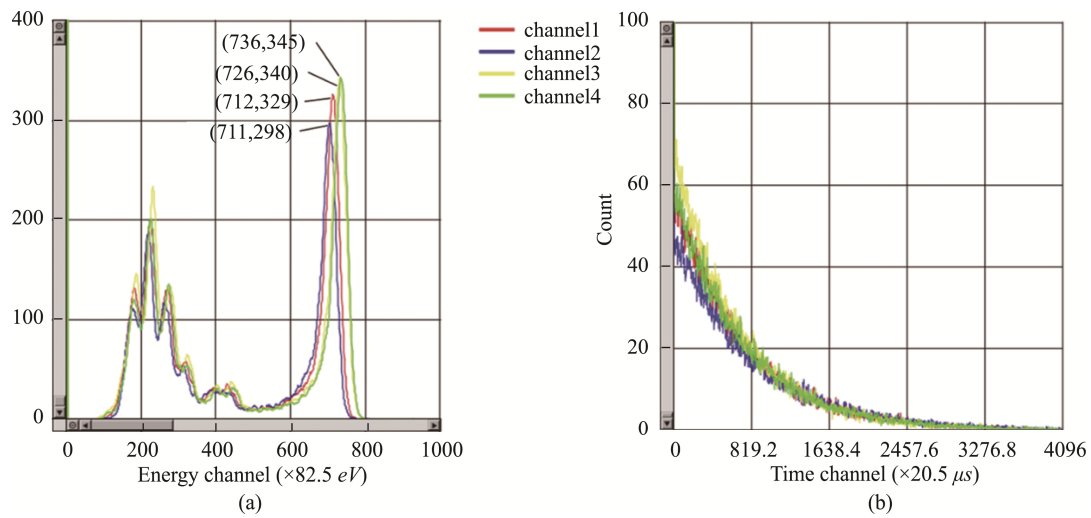


Fig.5 The Summery of Energy and Time Spectra of 4 pixels: (a) Energy Spectra, (b) Time Spectra

Table 1 Statistics of the Energy Spectra of Four Channels

Channel Number	Total Photon Count	Count of Full-energy Peak	Address of Full-energy Peak	FWHM	Energy Resolution
1	162816	41885	712	42	5.8%
2	162816	38497	711	43	6.0%
3	162816	45693	726	42	5.7%
4	162816	42041	736	39	5.3%

3.2 Test and Discussion of 2D Spectrum

The 2D spectrum of energy and time is the photon count distribution in a 2D plane that takes the particle energy as the X-axis and the time interval between particles as the Y-axis, as shown in Fig.6, in which the energy channel represents the photon energy, the time channel represents the interval time of photon emission, and the grade of color indicates the count value, i.e. the darker the color, the smaller the count value. Label (1), (2), (3) and (4) represent readout channel 1, 2, 3 and 4 respectively. The 2D spectra have 4096×4096 data points, however, to avoid too few or scattered data points, they are compressed to 100×100 in the actual graph, i.e. the energy channel unit is $2048/100$, and the time channel unit is $4096/100$.

Fig.6 (a), (b), (c) and (d) are the 2D spectra of 4 readout channels respectively. The results show that the characteristic peak of the energy spectrum can be seen

from the transverse distribution, and the address of the full energy peak is about 730. Meanwhile, from the longitudinal distribution, the exponential attenuation trend is obvious, and the time characteristics of each peak can be extracted respectively.

For further investigation on the distribution of the 2D spectrum, a three-dimensional (3D) histogram is drawn using the spectrum data of readout channel 1, as shown in Fig.7, keV and 0.8ms respectively. The 3D histogram displays the characteristic peaks more clearly, which reveals the exponential decay trend of the time distribution of each peak.

To quantitatively analyze the decay time of time spectra near the characteristic peaks, curve fitting is performed using the exponential decay curve. Fig.8 is the fitting result of the time spectrum of full energy peak located at 712 of readout channel 1, which has a rather high confidence level of 0.99. The time spectrum

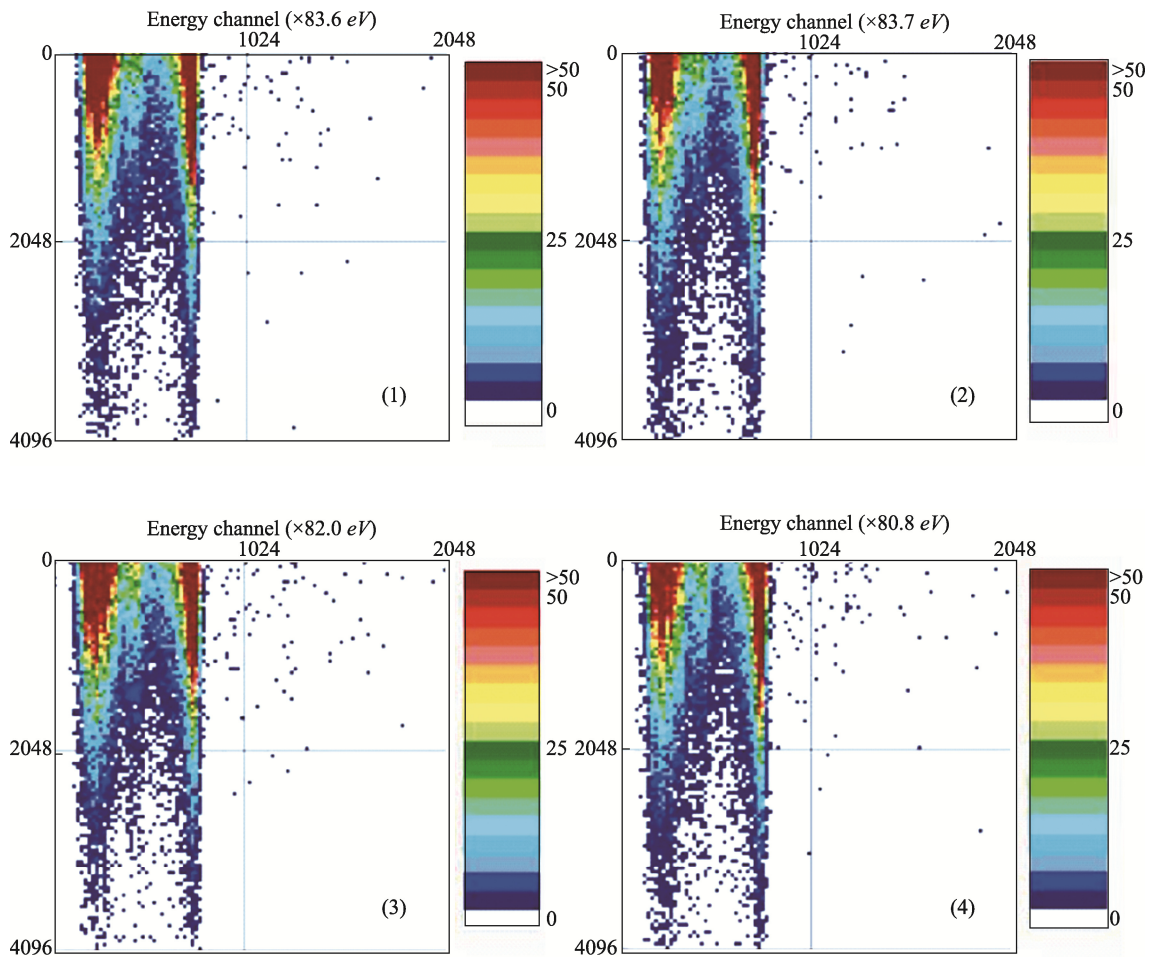


Fig.6 Two-dimensional Spectra of ^{241}Am Gamma Ray

data is derived from a cross section along the time axis of the full energy peak, and the fitting time constant is 18.5, corresponding to a time of 15.5 ms. The processing of other peaks is similar as this.

Table 2 shows the time constants obtained by curve fitting of the four characteristic peaks of readout channel 1, which are all around an average decay time of 15.26 ms.

The decay time constants of the characteristic peaks of four readout channels is plotted vs the energy peak address, as shown in Fig.9. It can be seen that the time constants of the five characteristic peaks of each readout channel are basically the same, while the time constants of different readout channels are slightly different, due to the difference between detector pixels and readout channels. The result agrees well with the

theoretic analysis as following.

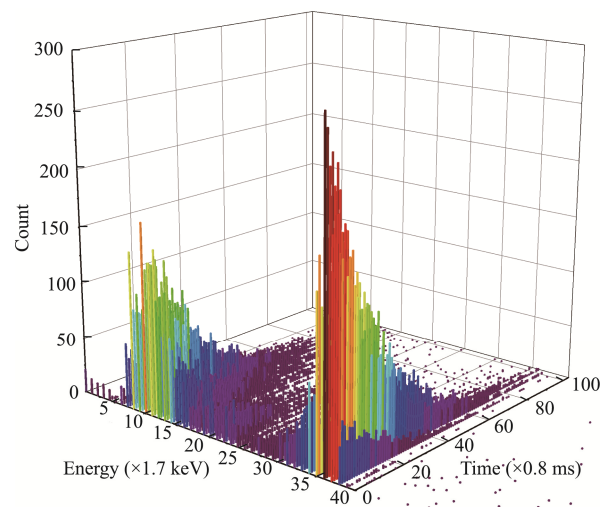


Fig.7 The 3D Histogram of the Energy and Time 2D spectrum

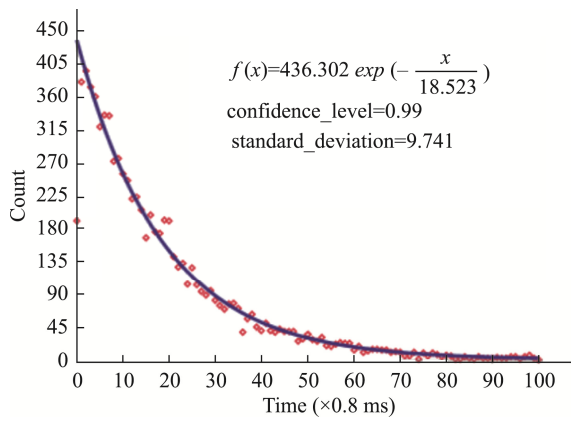


Fig.8 The Curve Fitting of Time Spectrum of the Full Energy Peak

Table 2 Statistics of the Time Spectra of the Characteristic Peaks of Channel 1

Characteristic Peaks	Peak Address	Energy/ keV	Time Constant	Decay Time/ms
Am γ 59.5keV	712	59.5	18.5	15.5
Am γ 26.3keV	315	26.3	17.9	15.0
N_p L_{α} 20.8keV	267	22.3	18.2	15.3
N_p L_{β} 16.8 / 17.8keV	219	18.3	18.4	15.4
N_p L_{α} 13.4keV	175	14.6	18.0	15.1

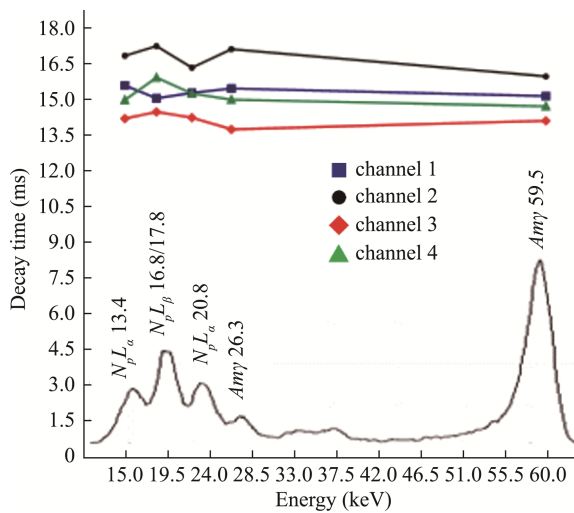


Fig.9 The Decay Time of ²⁴¹Am Energy Peaks

3.3 Theoretic Analysis of Time Spectra

Suppose the probability of photon emission, from

the radioactive source toward one pixel of the Gamma ray detector, is far less than 1 in a single time step, then the probability of n photon emission in a large number of time steps should be Poisson distribution function:

$$P(n) = \frac{\bar{n}^n}{n!} \exp(-\bar{n}) \quad (1)$$

where \bar{n} is the average photon numbers over the time. So during that time, the probability without photon emission is $P(0) = \exp(-\bar{n})$, and the probability with photon emission is $P_e = 1 - \exp(-\bar{n})$.

If the average period of photon emission is τ , then the probability of photon emission during a time t should be rewritten as

$$P_e(t) = 1 - \exp\left(-\frac{t}{\tau}\right) \quad (2)$$

Therefore, the photon emission rate at any time t should be

$$G(t) = \frac{d}{dt} P_e(t) = \frac{1}{\tau} \exp\left(-\frac{t}{\tau}\right) \propto \exp\left(-\frac{t}{\tau}\right) \quad (3)$$

The decay time constants represent the time interval between nuclear reactions or secondary processes in the radioactive source. Since the secondary processes are soon enough after the nuclear reactions, the record of each secondary process also represents the occurrence of a nuclear reaction. It means that the decay time constants of all kind of characteristic peaks should identically be the average period of nuclear reactions. Thus, the unit time yield of nuclear reaction can be estimated from the decay time constant. Note that, the response time (sub-micron second grade) of the Gamma detector and readout circuit is far less than the average time interval (mini-second grade) between nuclear reactions, so that it can be neglected in time measurement.

It is clear that the 2D spectrum of energy and time can reveal not only the energy information of radiation, but also the time information of radiation and the relationship between them, demonstrating a significant advantage of the 2D spectrum over the one-dimensional spectrum.

4 Conclusion

In this paper, a 4-channel 2D spectrum analysis system for energy and time is designed based on the pulse-width-modulation readout circuit, and the

system converts the radiation signal into a rectangular pulse, of which the pulse width corresponds to the energy of the particle and the rising edge represents the occurrence time. The pulse width, occurrence time, and pulse count of the rectangular pulse can be measured synchronously by the counter, thus the energy-and-time 2D spectrum of the radiation particles can be obtained by the bi-parameter statistics of the pulse count. The developed 2D spectrum system is tested with gamma rays from an ^{241}Am source, and the 2D spectra of energy and time are obtained as well as the independent energy and time spectra. The energy spectra of the four channels can give all the characteristic peaks of ^{241}Am gamma rays, and the energy resolution of 59.5keV full energy peak can reach 5-6%, indicating that the energy resolution and consistency of the system are good. Through the curve fitting of the time spectrum of the characteristic peaks, the time constant of each characteristic peak is obtained, and the time characteristics of the nuclear reaction of ^{241}Am isotopes are preliminarily revealed.

The 2D spectrum analysis system for an arrayed detector designed in this paper not only avoids the use of ADC device, but also avoids a large number of redundant data, and thereby improves the efficiency and speed of data processing. The system has the advantages of small size, low cost, strong scalability, and high energy and time resolution, providing a new way for the development of practical energy-and-time 2D spectrum analysis systems.

5 Acknowledgments

This work was supported by the National Natural Science Foundation of China (Grant No. 61274048) and the National Science Associated Foundation of China (Grant No. 10876044).

References

- [1] Gerardi G. and AbbeneL. (2014). A digital approach for real time high-rate high-resolution radiation measurements. *Nuclear Instruments and Methods in Physics Research A*, 768, PP.46-54.
- [2] Lee P. S., Lee C. S. and Lee J. H. (2013). Development of FPGA-based digital signal processing system for radiation spectroscopy, *Radiation Measurements*, 48, PP.12-17.
- [3] Shefali S. and Ayman I. H. (2020). Digital pulse deconvolution with adaptive shaping for real-time high-resolution high-throughput gamma spectroscopy, *Nuclear Instruments and Methods in Physics Research A*, 954, PP.161288 1-5.
- [4] Yinyu L., Hao X., Chunhui D., Chaoyang Z., Quanfeng Z. and Shun L. (2020). Real-time signal processing in field programmable gate array based digital gamma-ray spectrometer, *Review of Scientific Instruments*, 91, PP. 104707 1-10.
- [5] Geronimo G. D., Vernon E., Ackley K., Dragone A., Fried J., O'Connor P., He Z., Herman C., and Zhang F.(2008). Readout ASIC for 3D Position-Sensitive Detectors. *IEEE Transactions on Nuclear Science*, 55, PP.1593-1603.
- [6] Zhang F. and He Z. (2006). New Readout Electronics for 3-D Position Sensitive CdZnTe/HgI₂ Detector Arrays. *IEEE Transactions on Nuclear Science*, 53, PP.3021-3027.
- [7] Fiutowski T., Koperny S., Łach B., Mindur B., Świentek K., Wiacek P. and Dabrowski W. (2017). ARTROC - a readout ASIC for GEM-based full-field XRF imaging system. *Journal of Instrumentation*, 12, PP.C12016 1-9.
- [8] Parl C., Larue H., Streun M., Ziemons K. and Waasen S. van. (2012). Fast Charge to Pulse Width Converter for Monolith PET Detector, *IEEE Transactions on Nuclear Science*, 59, PP.1809-1814.
- [9] Kasinski K., Kleczek R., Grybos P. and Szczygiel R. (2012). Time-over-Threshold Processing Implementation for Silicon Detectors with Large Capacitances. In: *2012 IEEE Nuclear Science Symposium and Medical Imaging Conference Record (NSS/MIC)*. PP.882-885. Available at: <https://doi.org/10.1109/SSMIC.2012.6551232>.
- [10] Akashrup B., Michael W., Marta P., Andrew M., Henning H., Henning S., Helena M. A., Nikolaus K., Magda G., Jürgen G. (2022). Analog front-end for FPGA-based readout electronics for scintillation detectors, *Nuclear*

Instruments and Methods in Physics Research A, 1028, PP.166357 1-7.

- [11] The energy spectrum of ^{241}Am . Available at: <https://gammaray.inl.gov/SiteAssets/catalogs/ge/pdf/am241.pdf>.
- [12] Bell S. J., Baker M. A., Duarte D. D., Schneider A., Sella P., Sellin P. J., Veale M. C. and Wilson M. D. (2017). Performance comparison of small-pixel CdZnTe radiation detectors with gold contacts formed by sputter and electroless deposition. *Journal of Instrumentation*, 12, PP.P06015 1-10.

Author Biographies



ZHANG Liuqiang received Ph.D. from Shanghai Institute of Microsystem and Information Technology, Chinese Academy of Science in 2000. He is currently an associate professor in Optoelectronic Engineering College at Chongqing University. His main research interests include semiconductor radiation detectors, readout circuits and related systems.

E-mail: zlq@cqu.edu.cn



Copyright: © 2022 by the authors. This article is licensed under a Creative Commons Attribution 4.0 International License (CC BY) license (<https://creativecommons.org/licenses/by/4.0/>).